

Current Challenges of Complex Terrain Flow Research

Peter G Baines

Dept of Infrastructure Engineering

University of Melbourne

A complex and many-faceted topic. Some aspects:

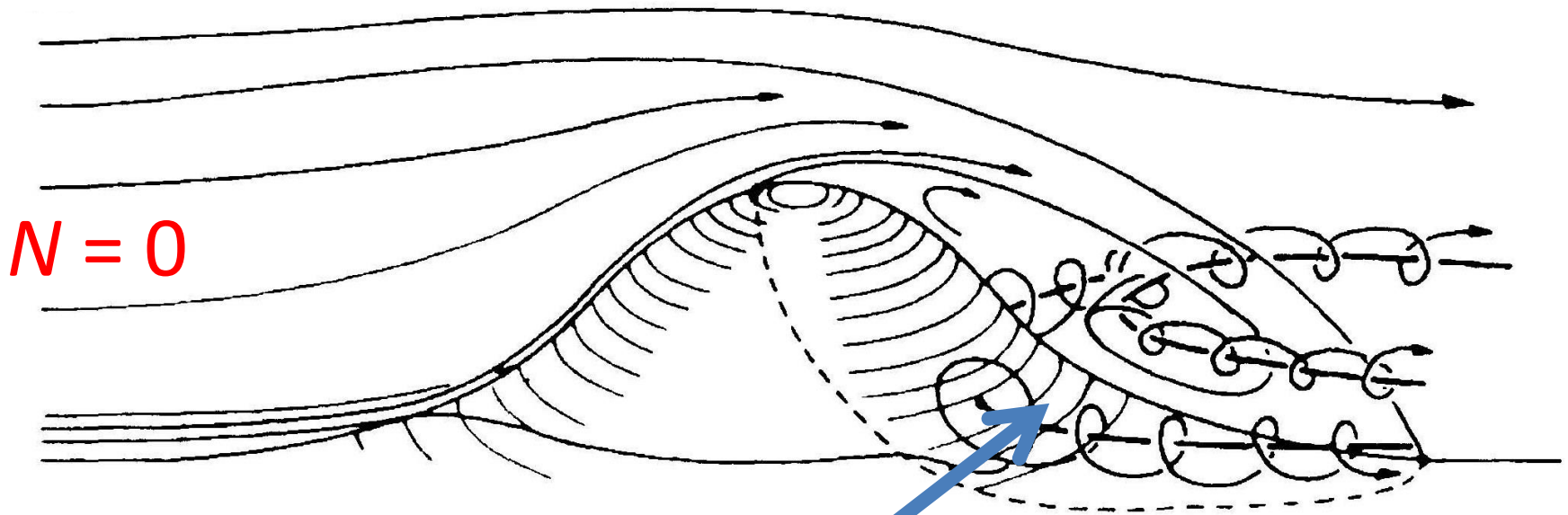
1. Interaction of density-stratified flow with topography
2. The effect of diurnal heating and cooling
3. The process of orographic frictional and wave drag
4. The effect of different surfaces, - snow, ice, vegetation and evaporation
5. - - - - -

Here I will address the first topic only. Some progress was made in the 1980s & 1990s . Since then, work has concentrated on field experiments (which tend to be site-specific) and numerical parametrisation.

Lab experiments have contributed a lot, and I think can contribute more.

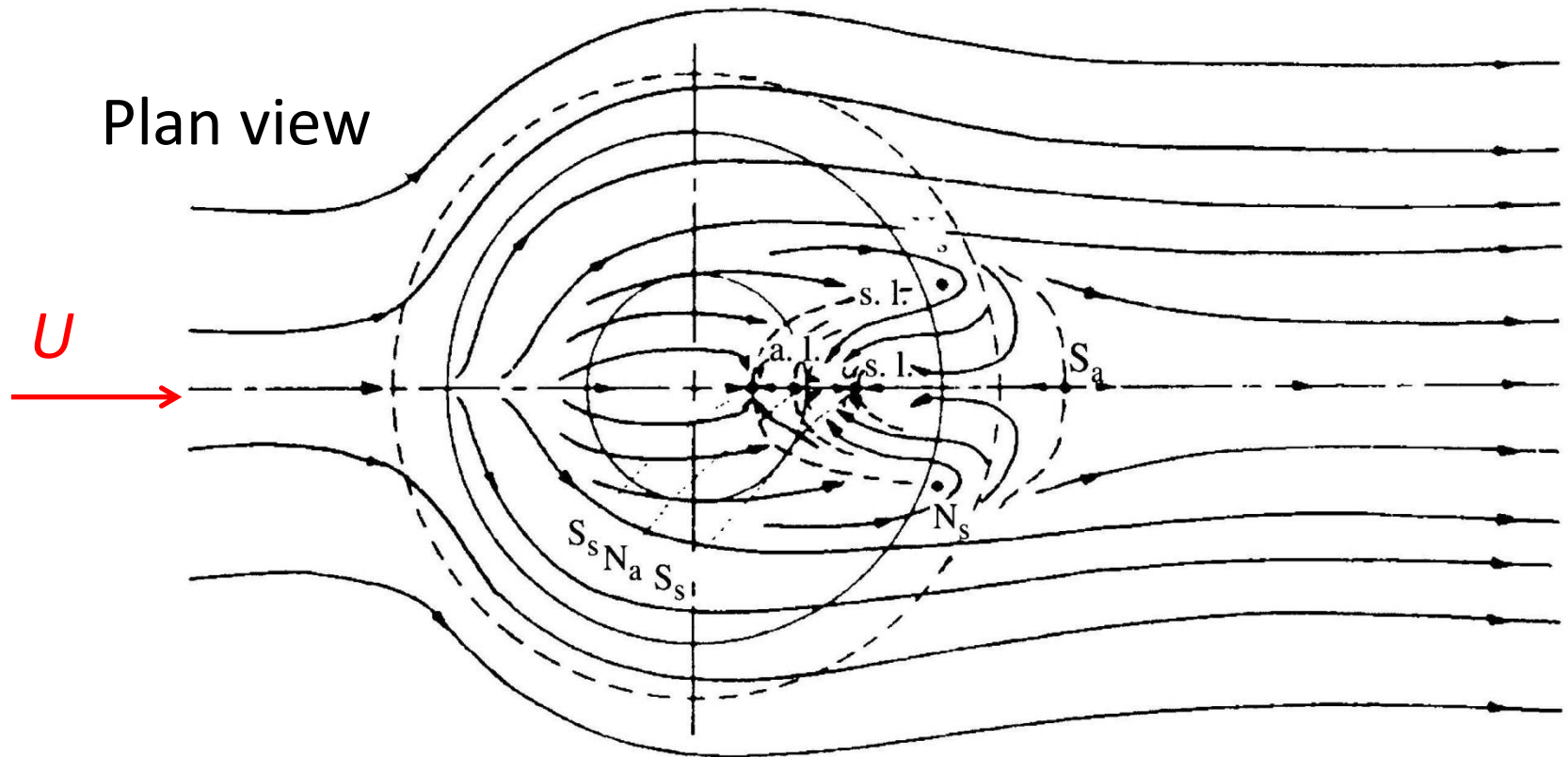
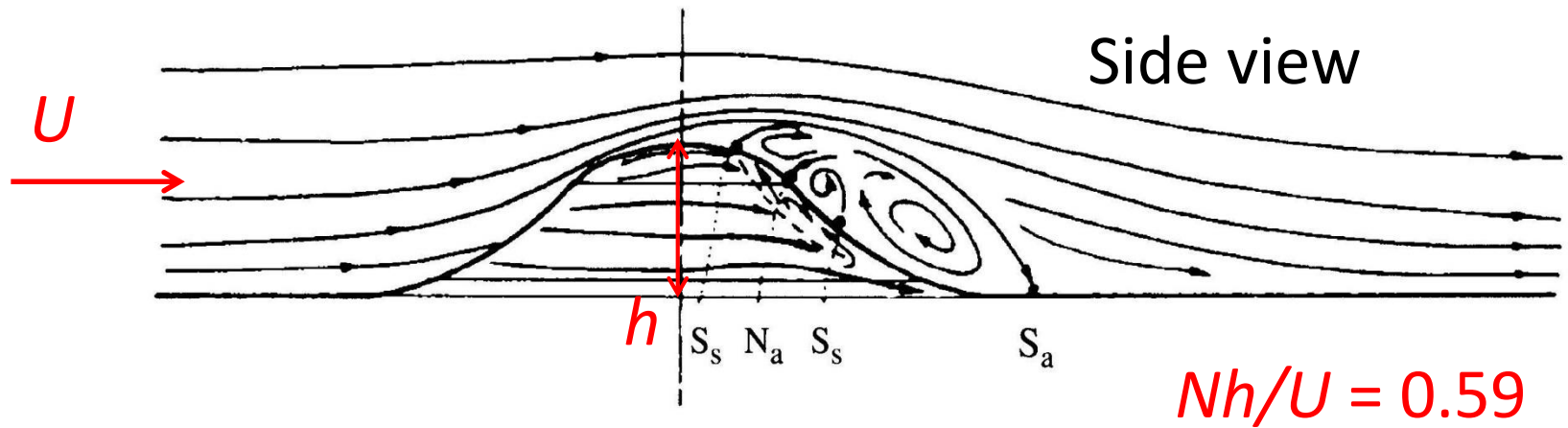
To understand flow in complex terrain, we need to start with flow past isolated topography.

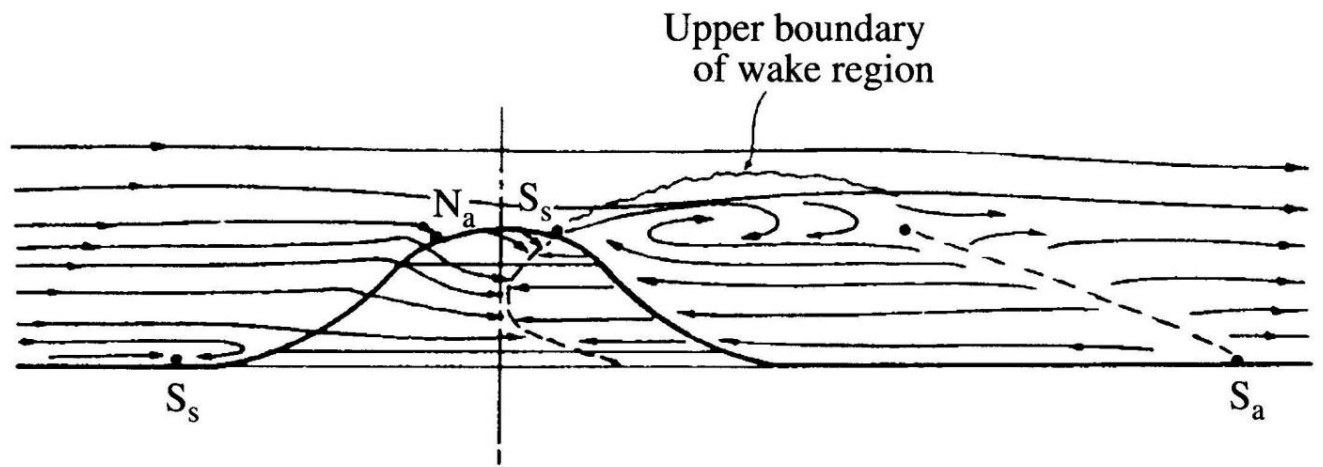
With no stratification, steady flow over an isolated hill looks like this:



Double horseshoe vortex wake

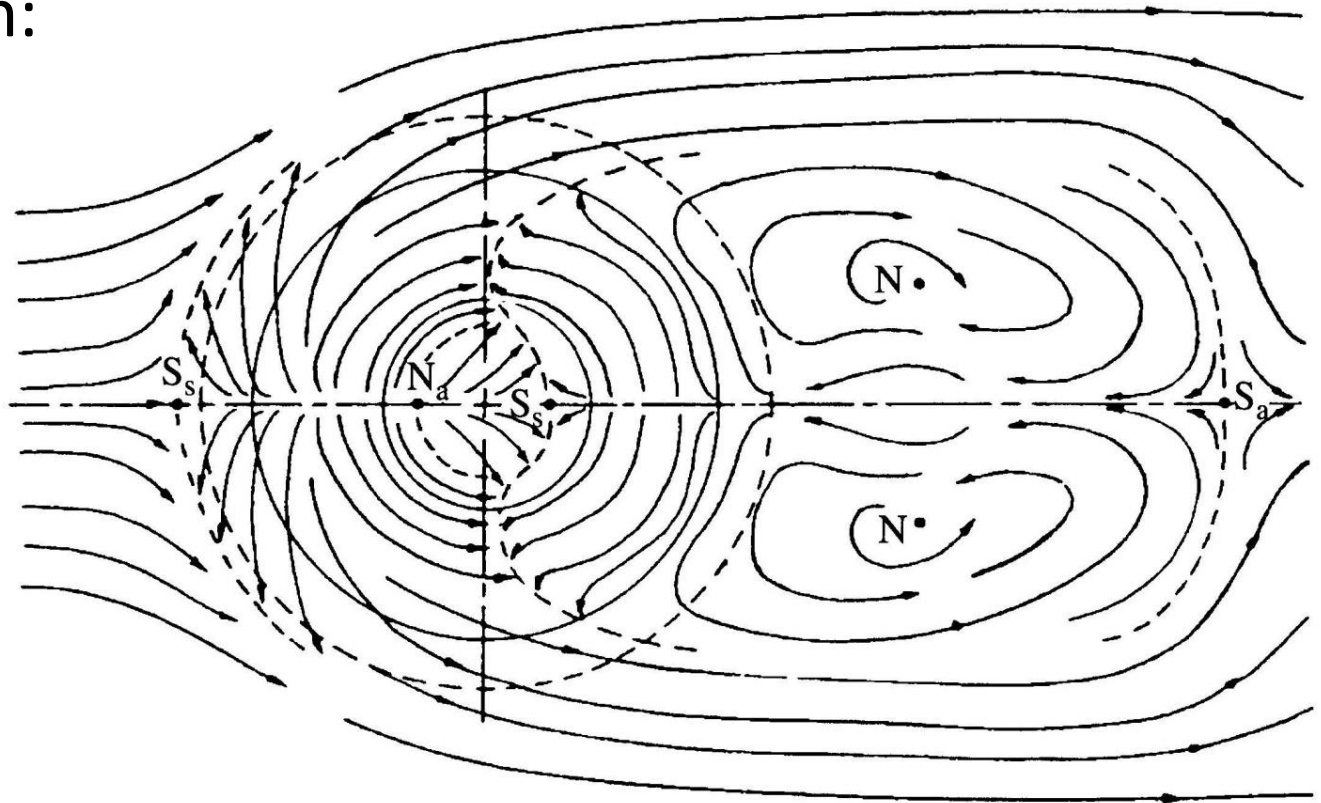
And with weak stratification it looks like this -



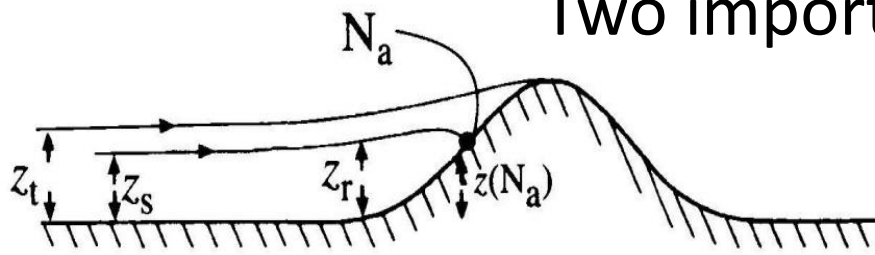


And with strong stratification:

$$Nh/U = 5$$

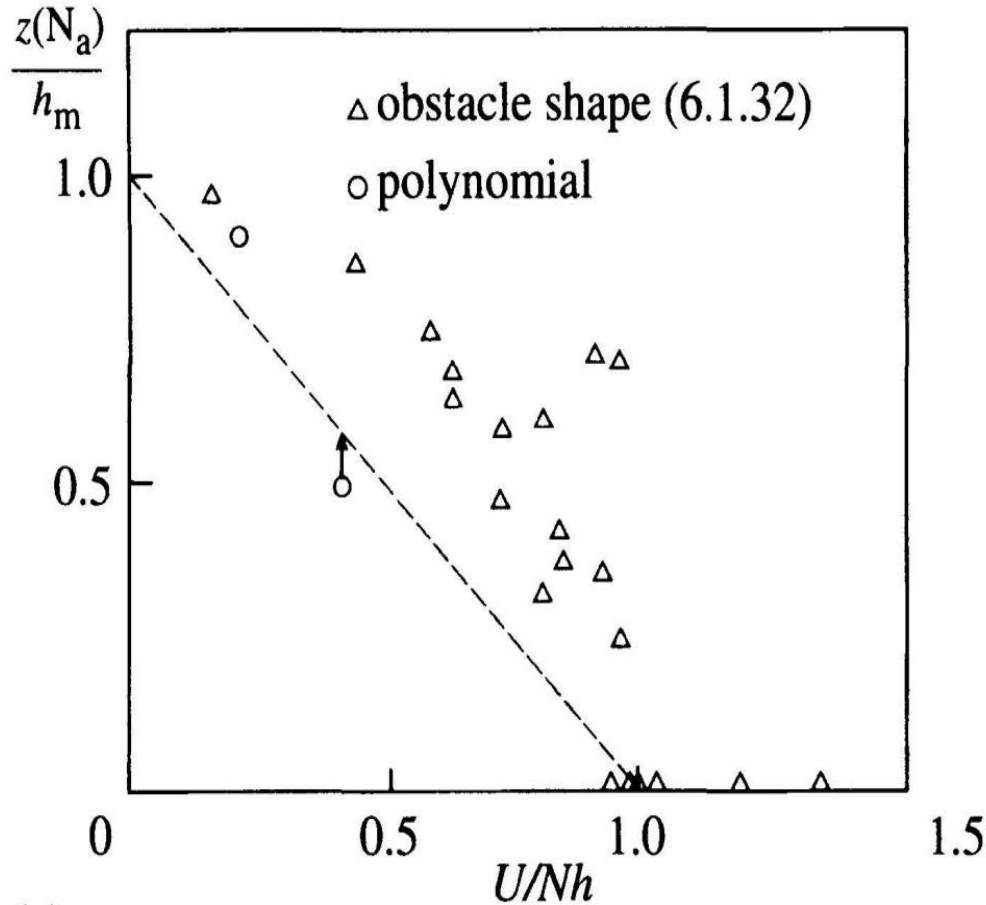


Two important levels: z_t and $z(N_a) = z_s$

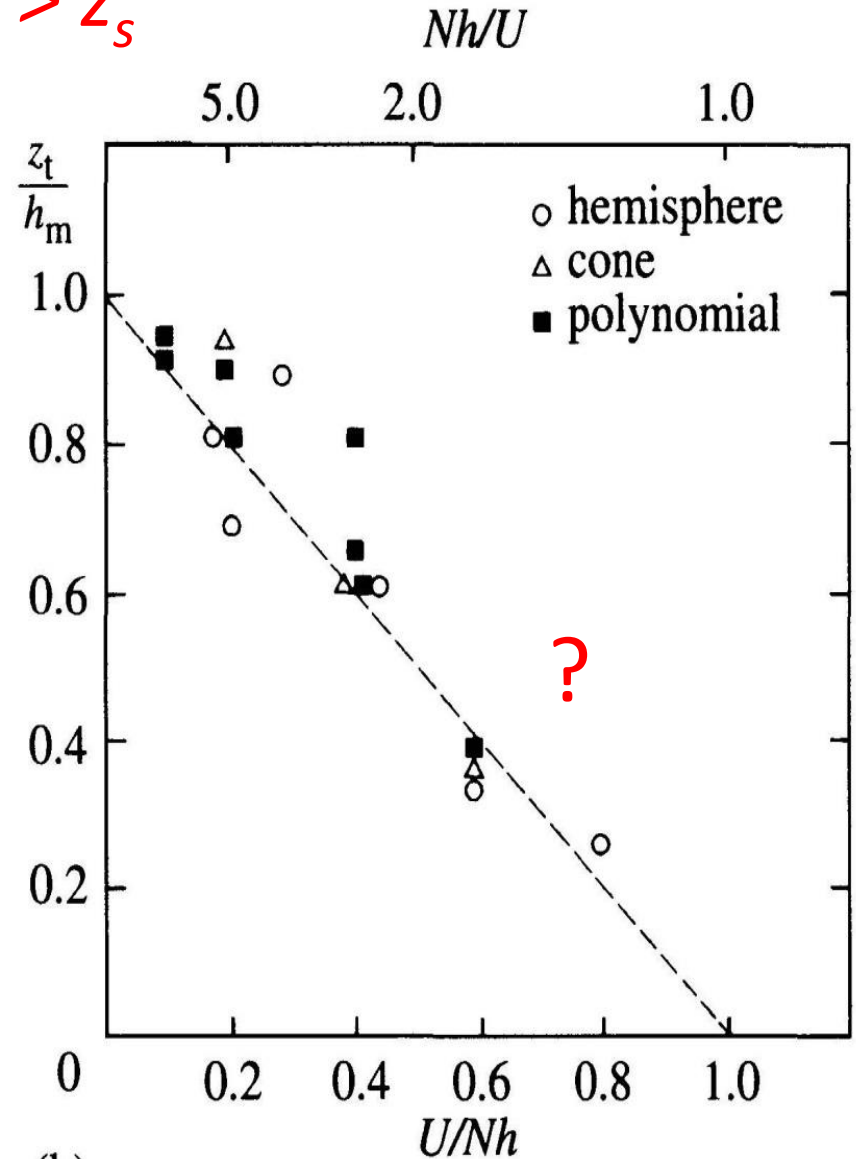


$$z_t > z_s$$

Axisymmetric obstacles



(Baines)

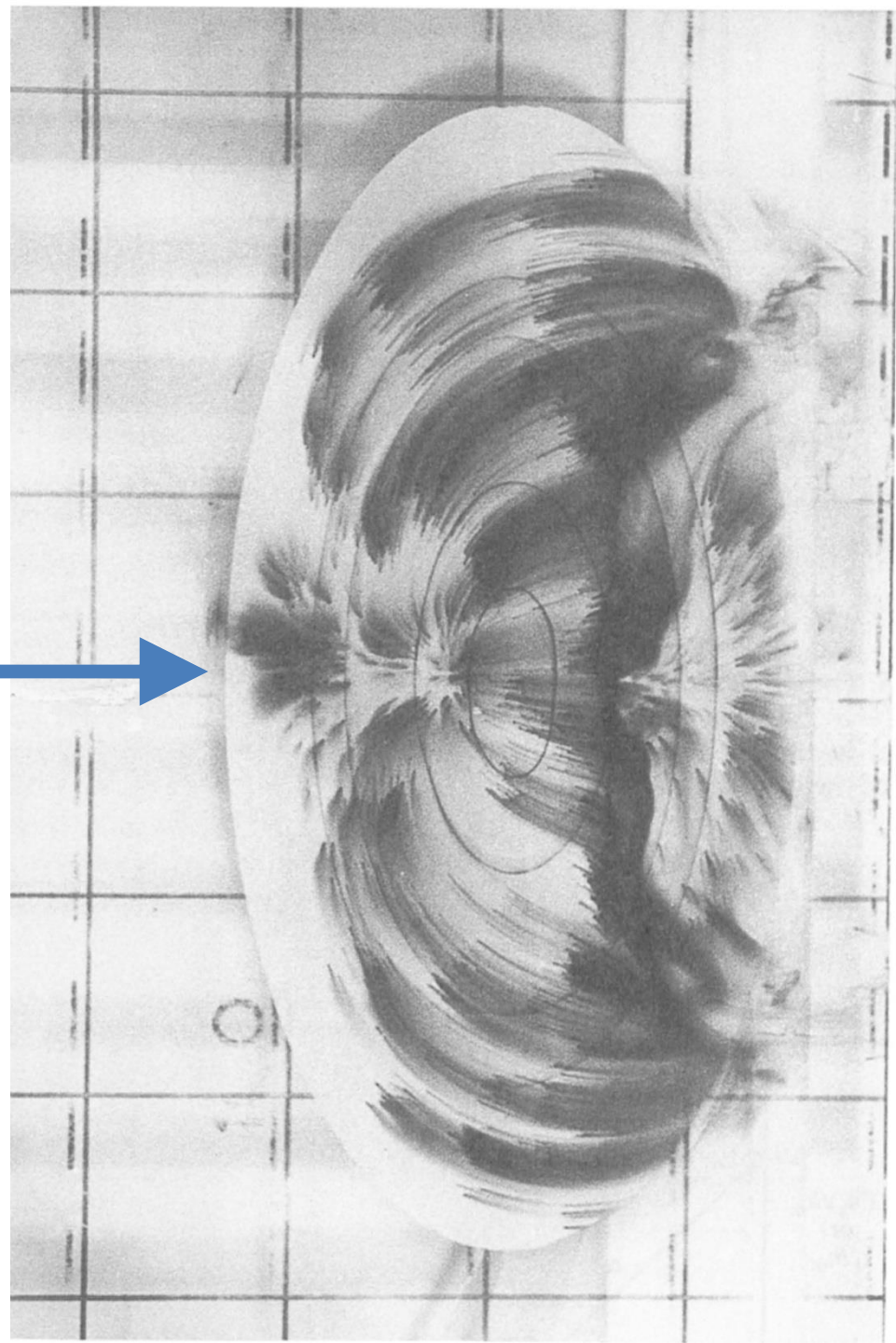


(Snyder, Britter & Hunt 1980)

Steady flow on the
surface of an
elliptical obstacle

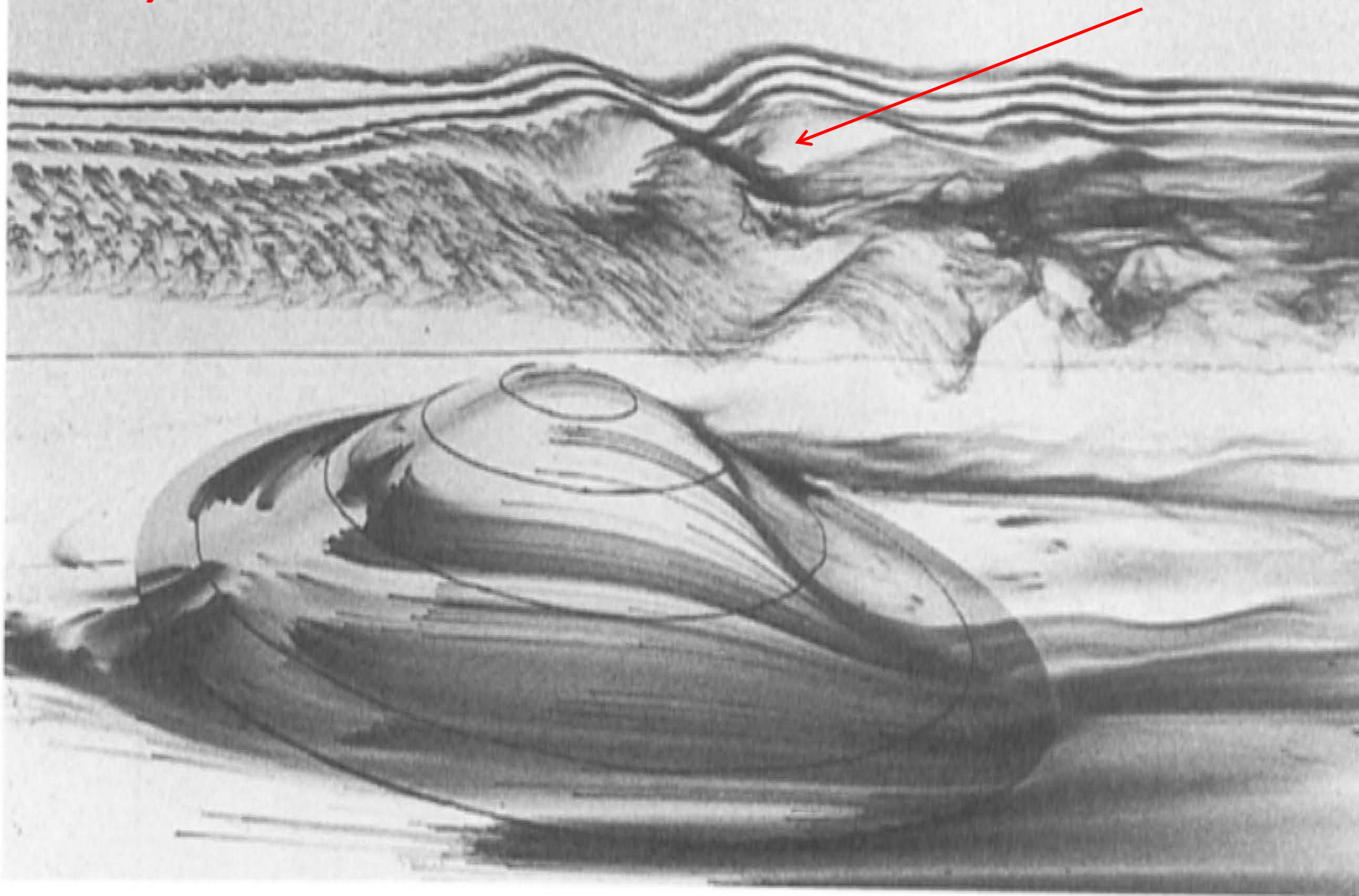
$$Nh/U = 3.45$$

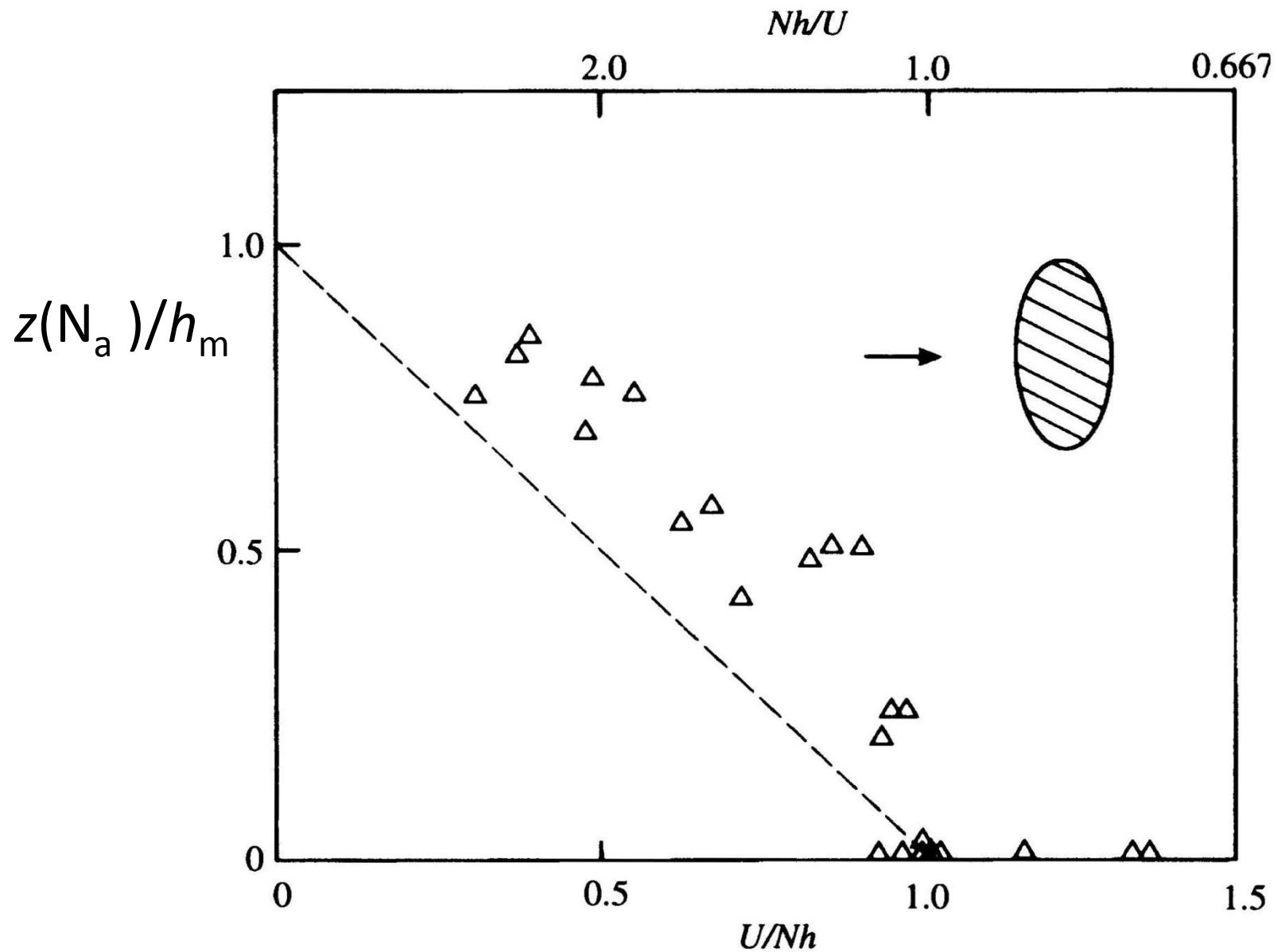
$$(U/Nh=0.29)$$



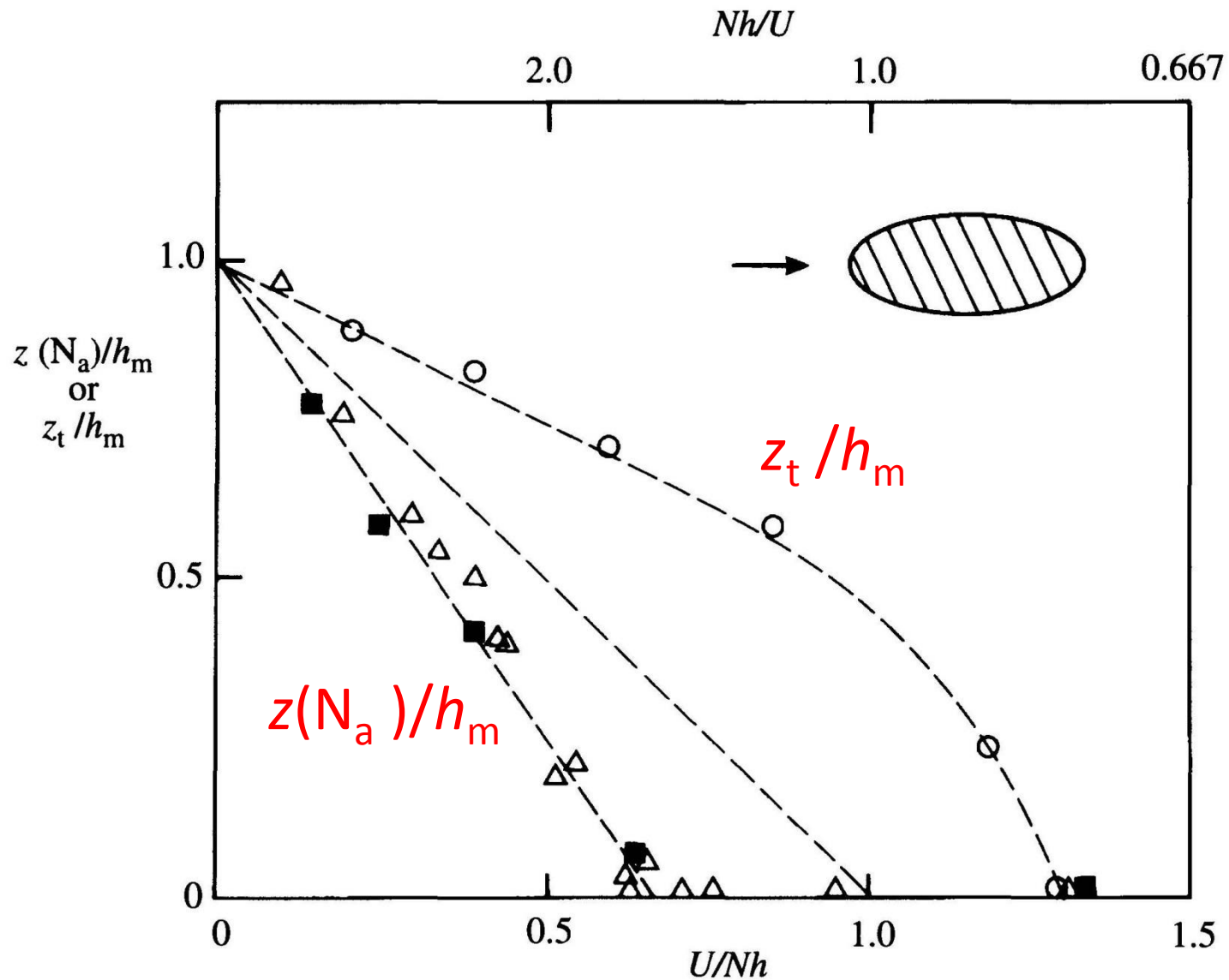
$$Nh/U = 2.5$$

In vertical plane above centreline



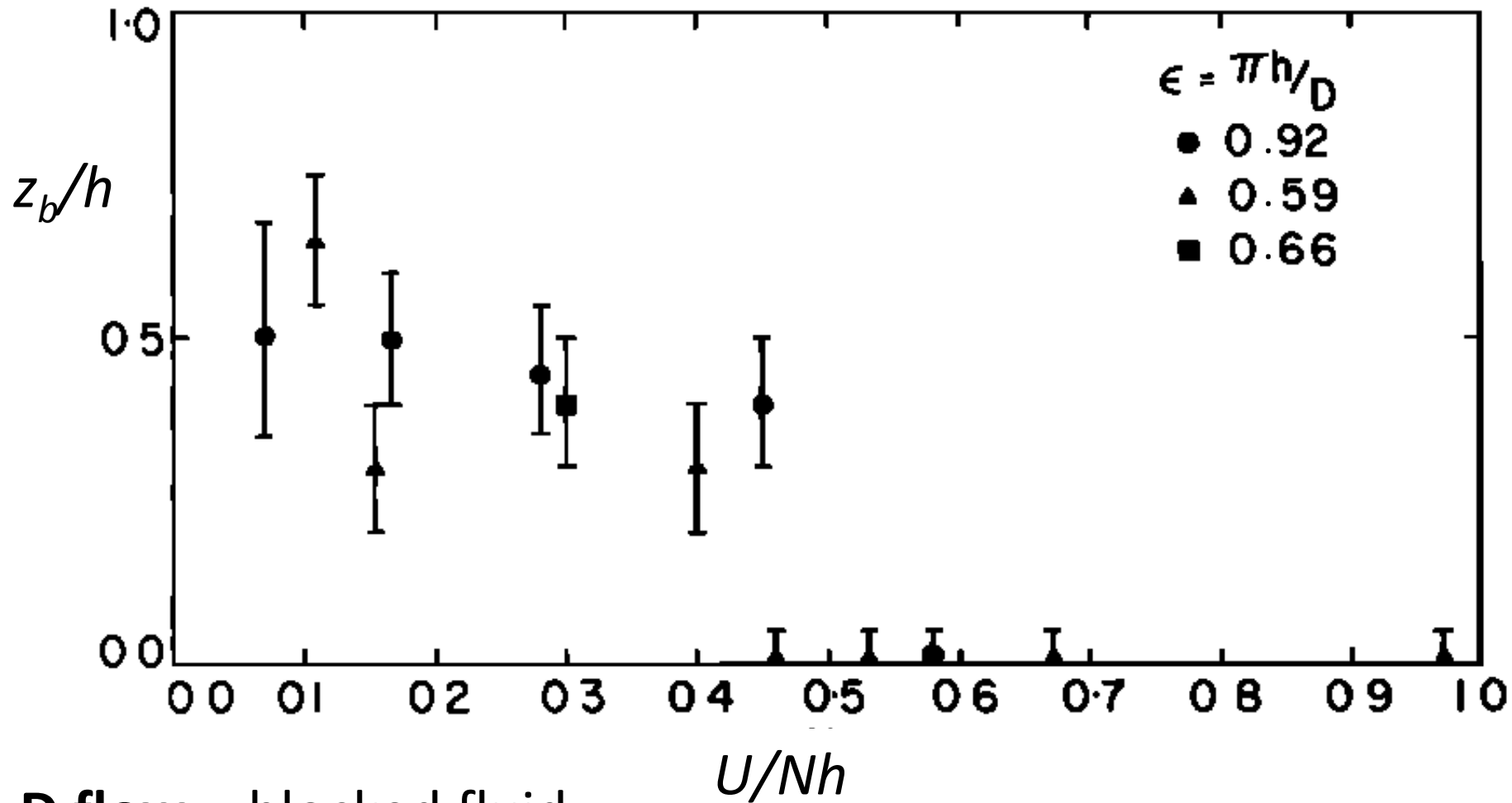


Height of the front –side stagnation point (N_a – node of attachment) for the “elliptical obstacle”

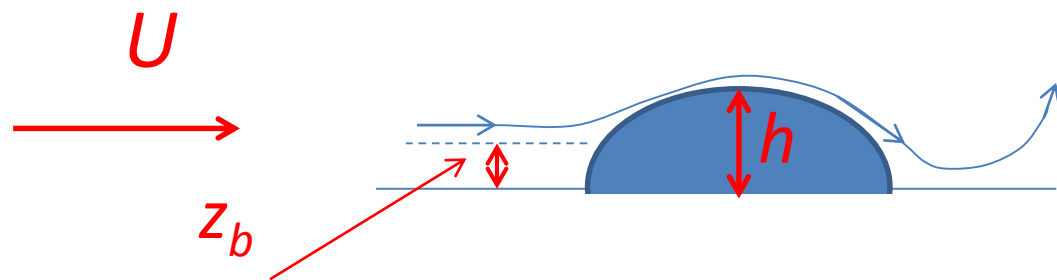


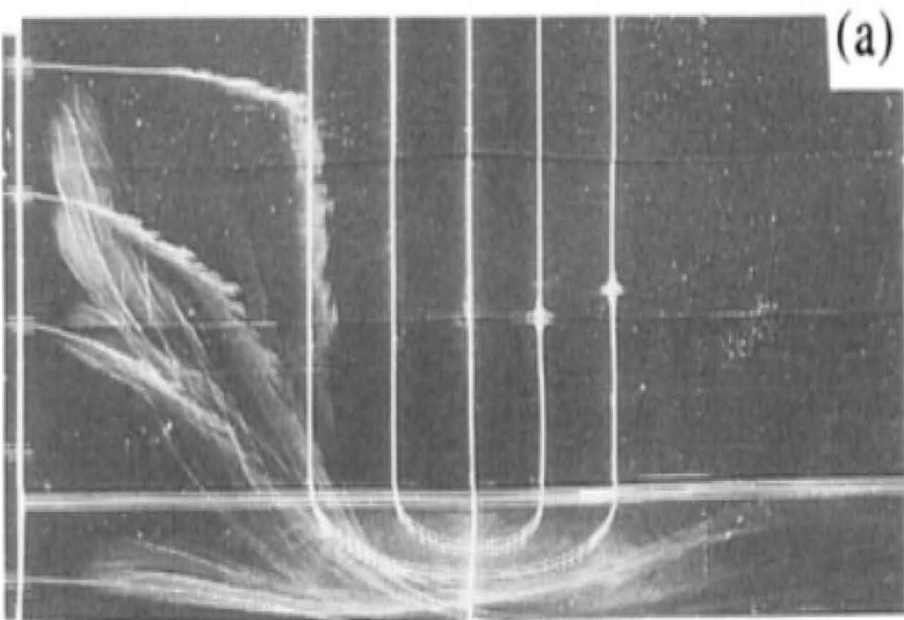
$z(N_a)$ and z_t for the same “elliptical obstacle” but placed “end on”

From Baines & Smith (1993)

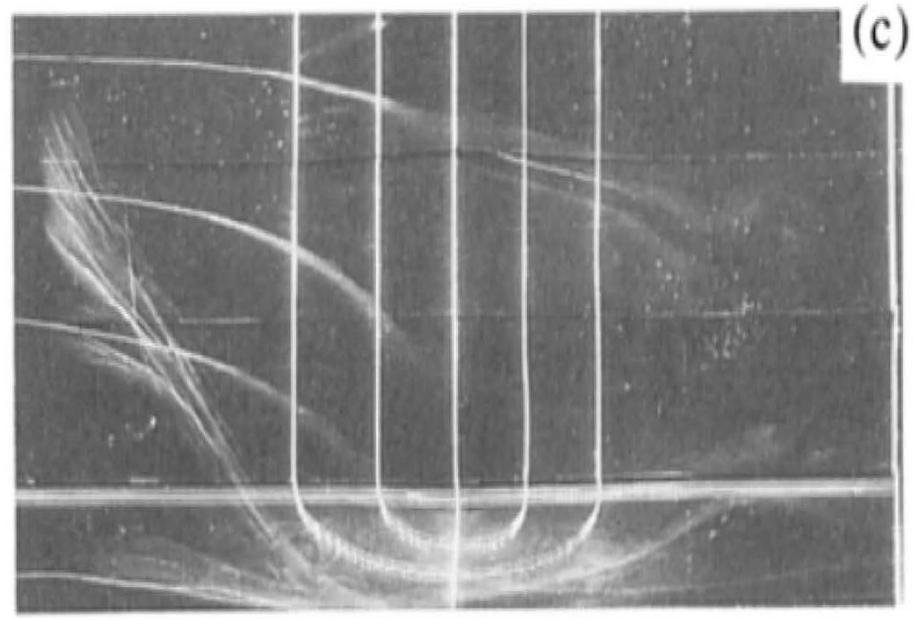


2-D flow - blocked fluid
 for $Nh/U > 2$



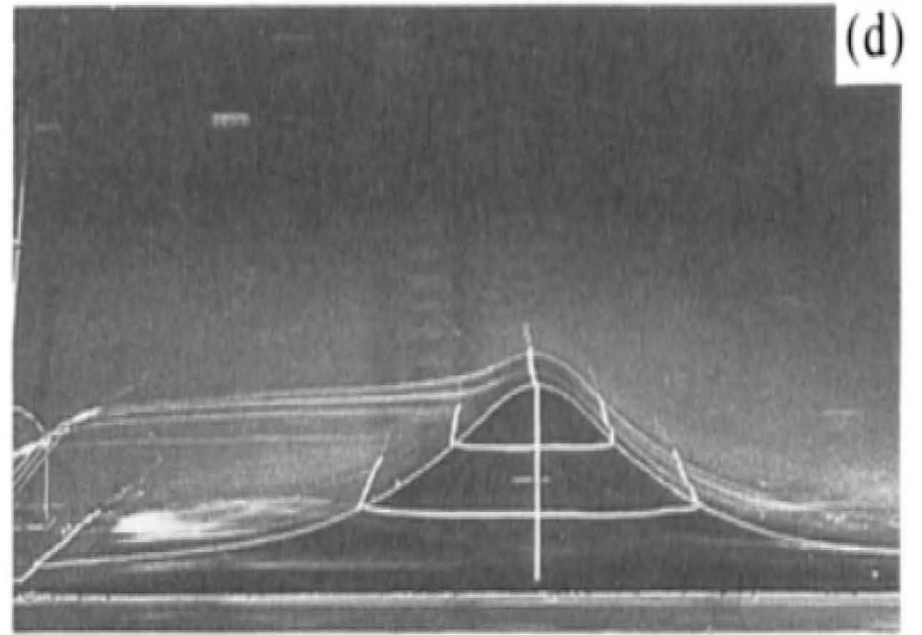
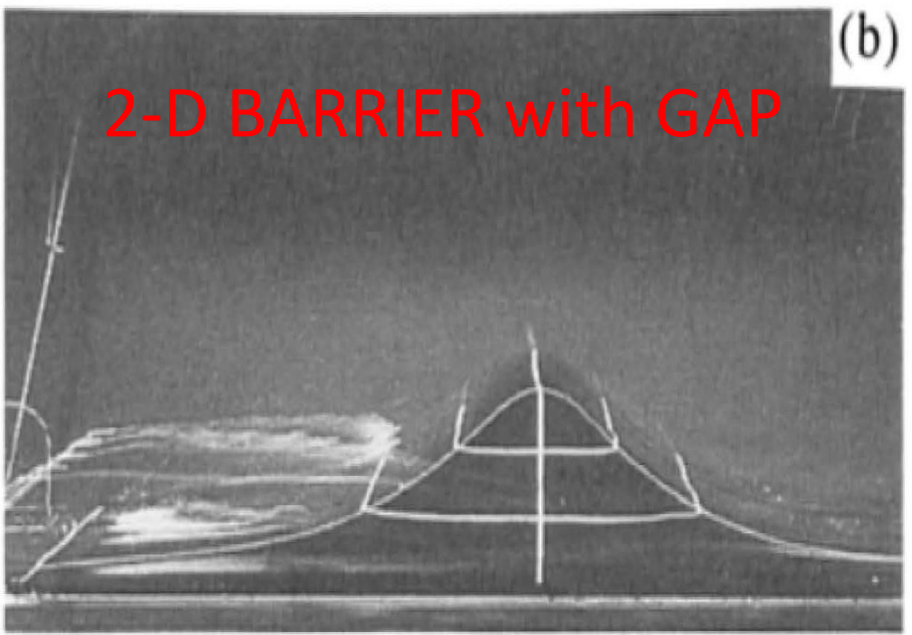


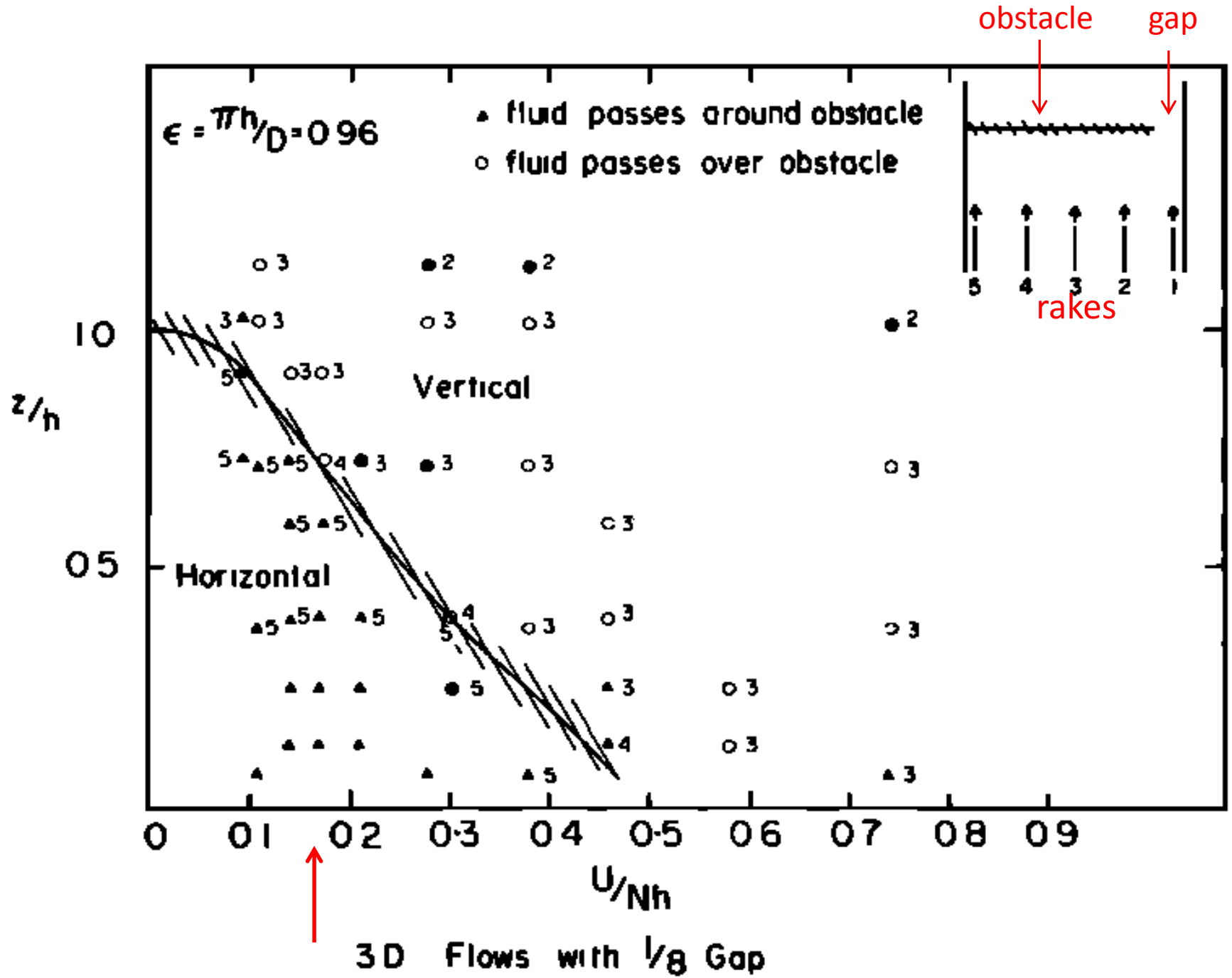
Low level rake



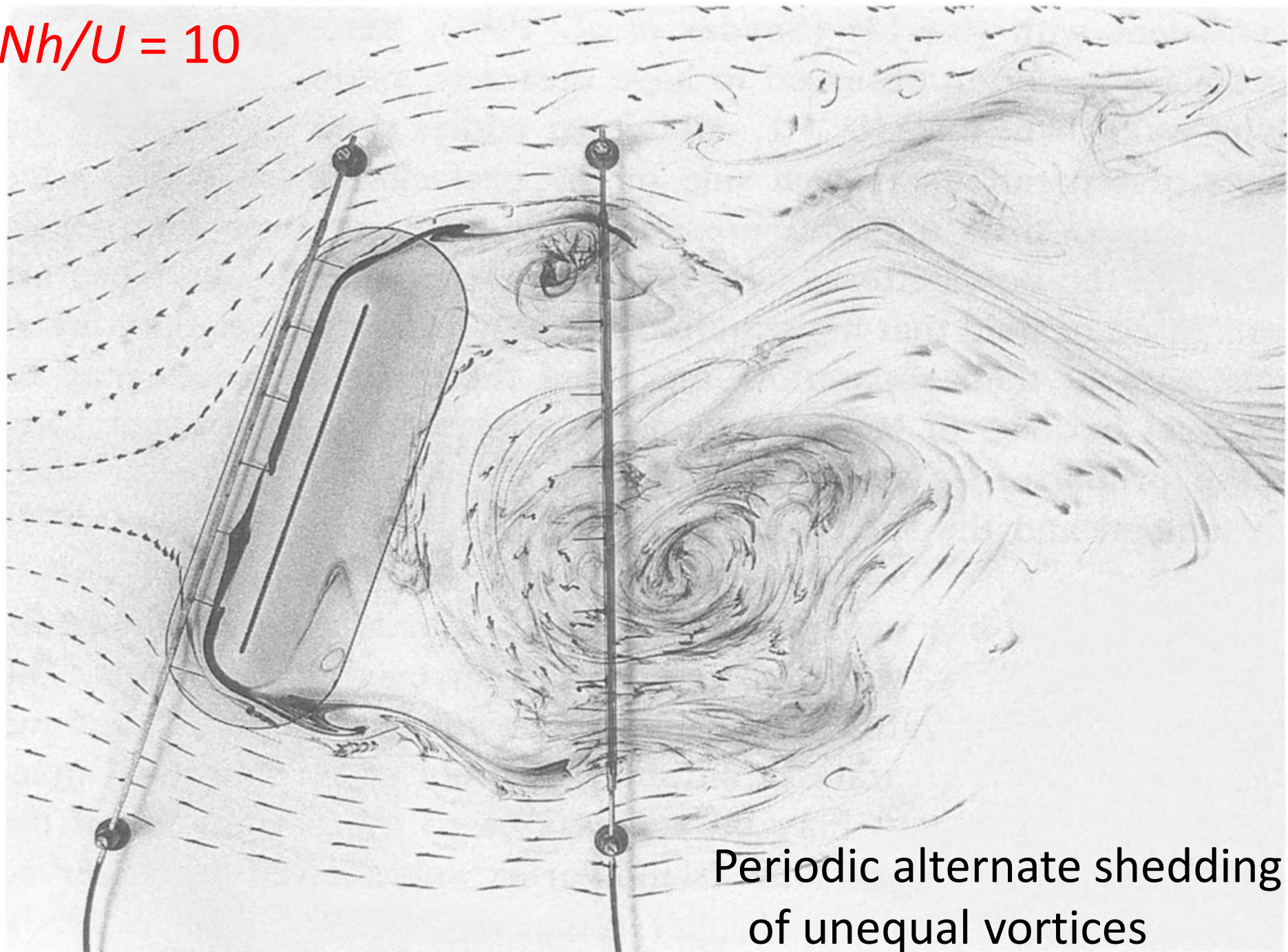
Higher level rake

$Nh/U = 5.9$

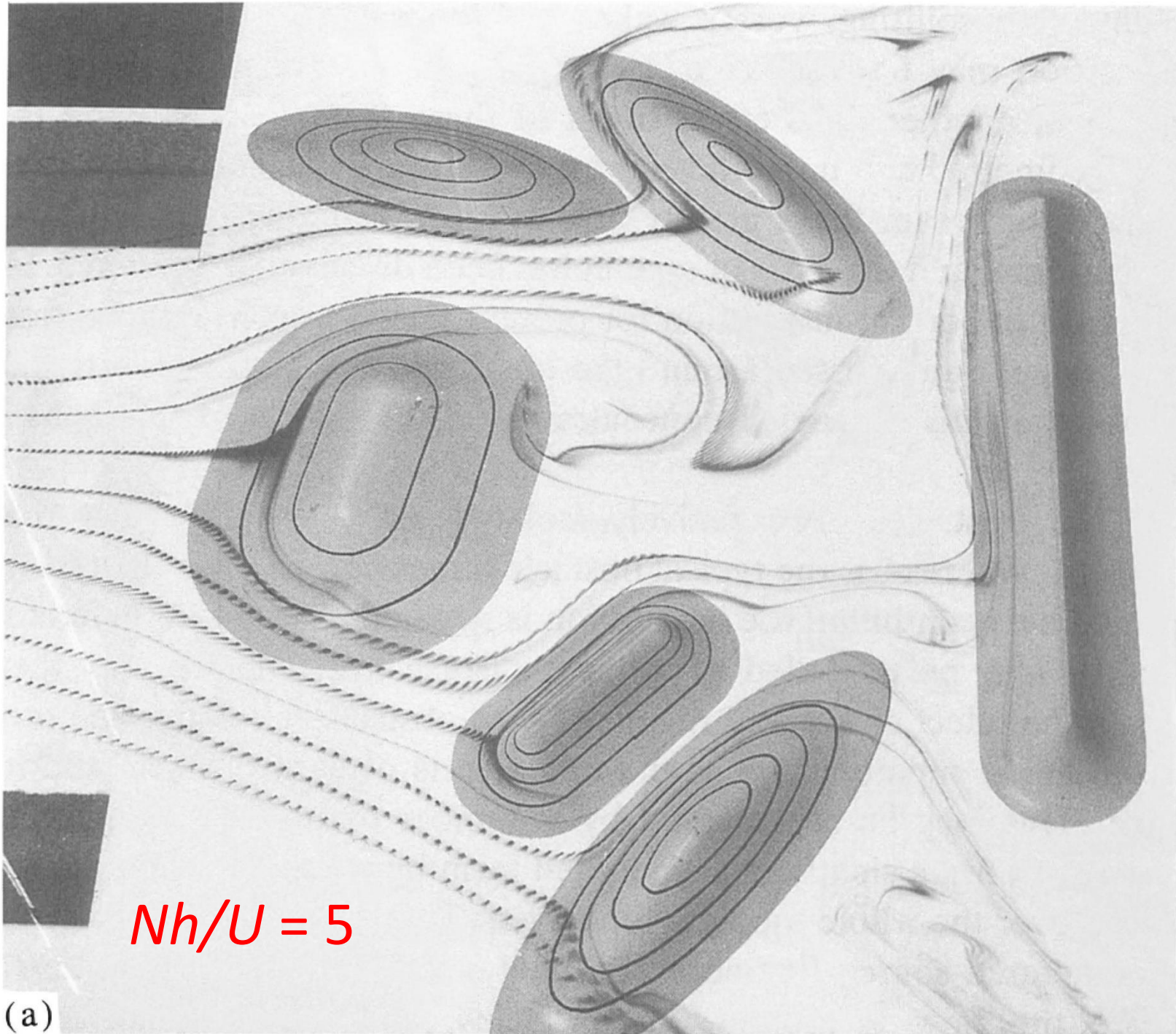




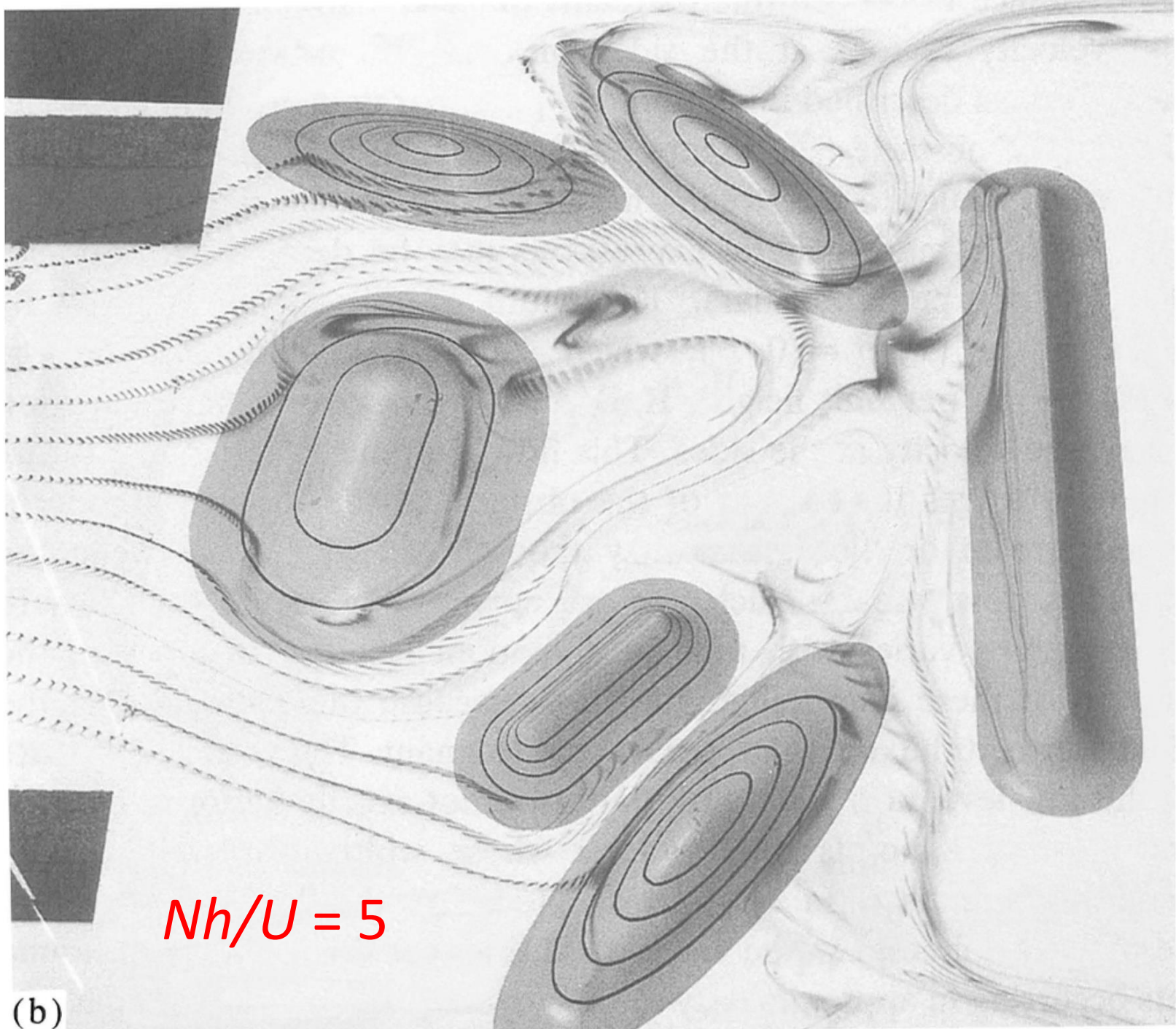
$Nh/U = 10$



Periodic alternate shedding
of unequal vortices



(a)



$Nh/U = 5$

(b)

In Conclusion –

Flow through complex terrain is complex, and may well contain unpredictable variability. But we can at least understand it (and make progress in doing so) by considering simple situations and proceeding to more complex ones.

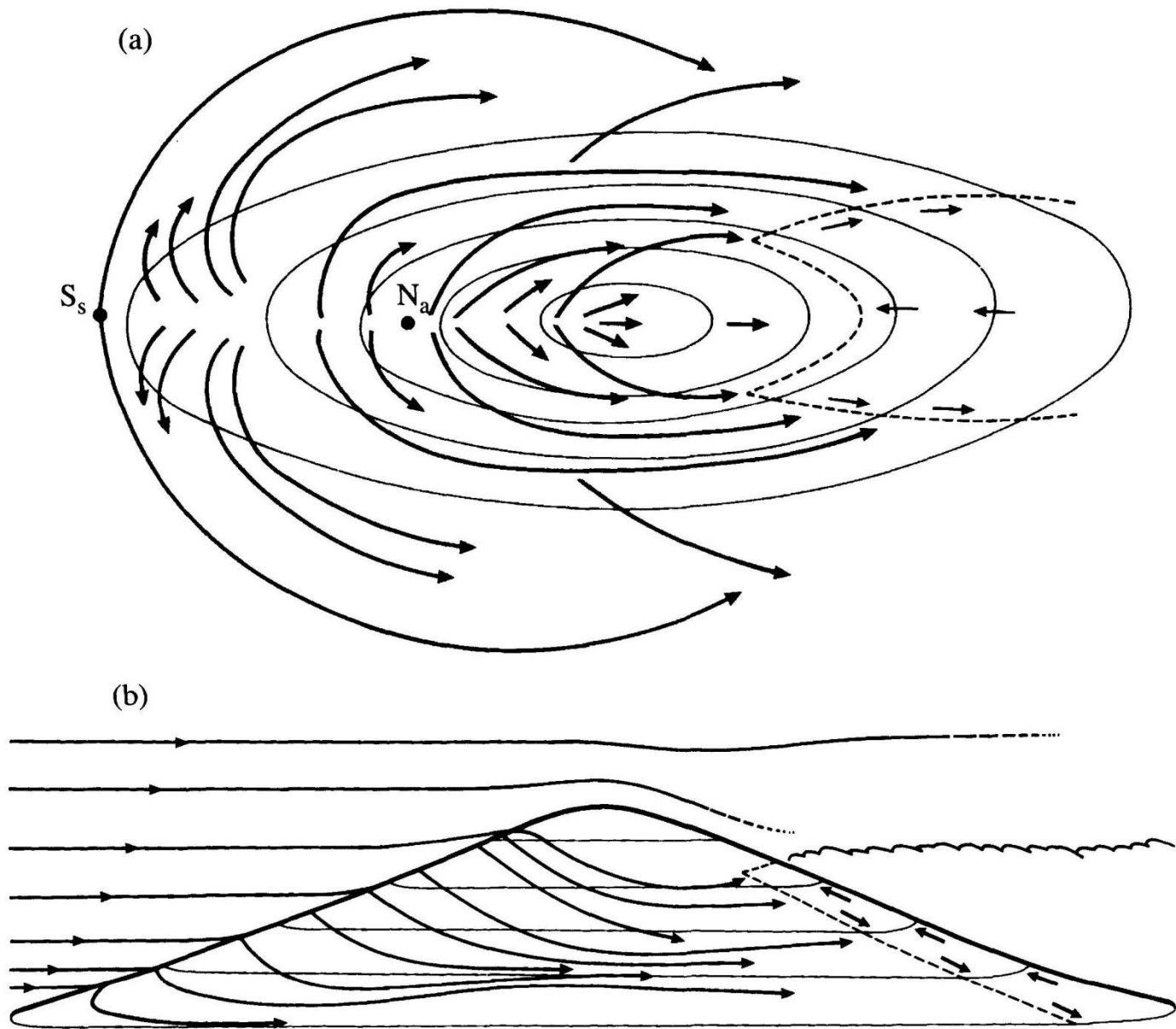


Fig. 6.32. Sketches of the flow pattern on the surface and on the vertical plane of symmetry for flow past an obstacle elongated in the downstream direction of the form (6.1.15) with $\nu = 3/2$ and $b/a = 0.38$, for $Nh/U = 4.2$, $R_e = 430$. (a) Plan view of flow on the surface; (b) side view. (cf. Figures 6.26, 6.27.)

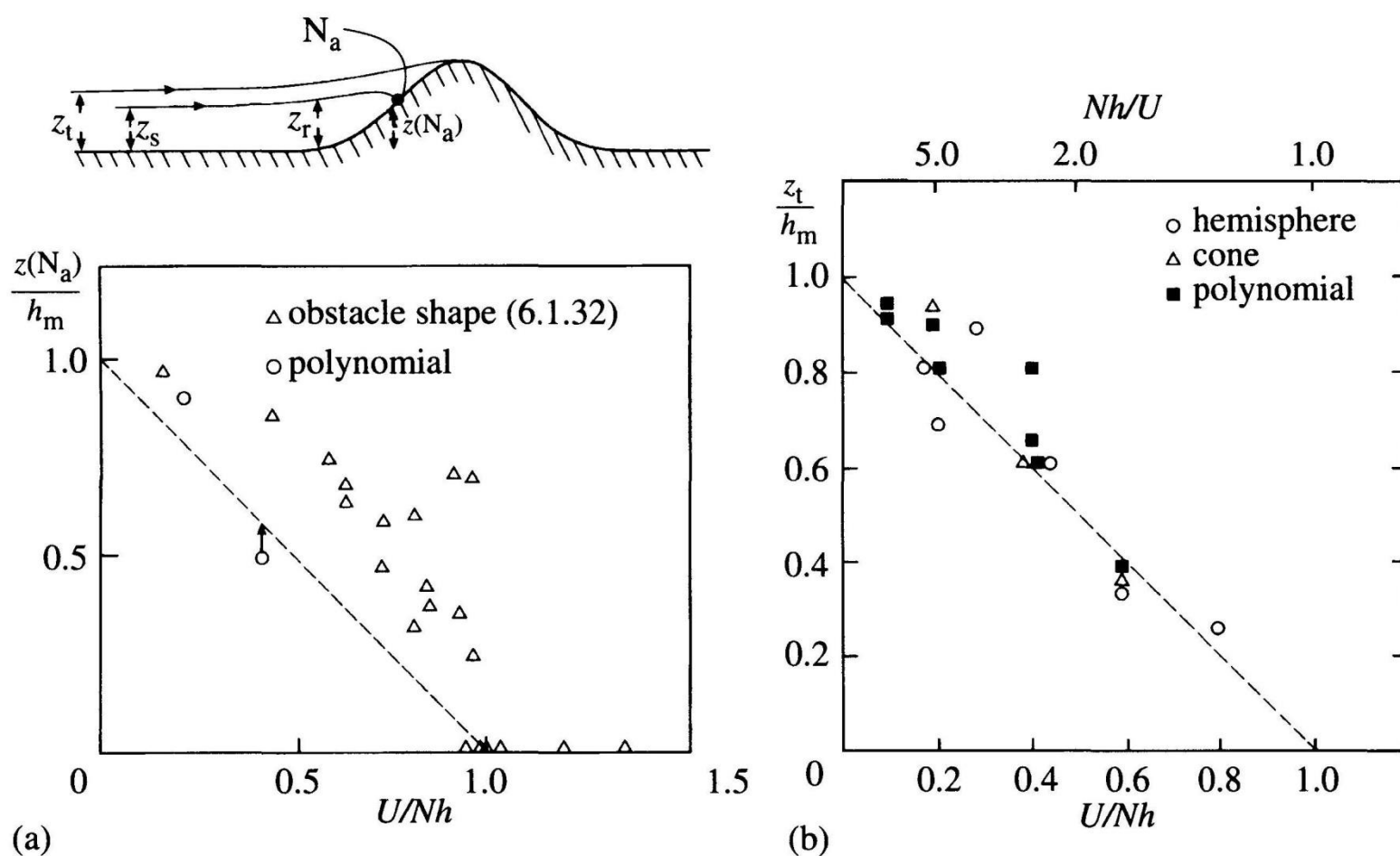


Fig. 6.29. (a) Observed height $z(N_a)$ of the stagnation point N_a on the upstream centre-line, as a function of Nh/U . Δ : obstacle shape (6.1.32); \circ : “polynomial hill” of Figure 6.22. A value of zero implies that no stagnation point exists. The dashed line denotes the relation $z(N_a)/h_m = 1 - U/Nh_m$. (From Baines & Smith 1993.) (b) The observed height z_t far upstream of the lowest streamline that reaches the crest of the obstacle, in terms of Nh/U , for a range of axisymmetric obstacle shapes. Δ : cone, $h/A = 0.66$; \blacksquare : “polynomial hill” of Figure 6.22, $h/A = 0.88$; \circ : hemisphere, $h/A = 1$. (From Snyder *et al.* 1980.)

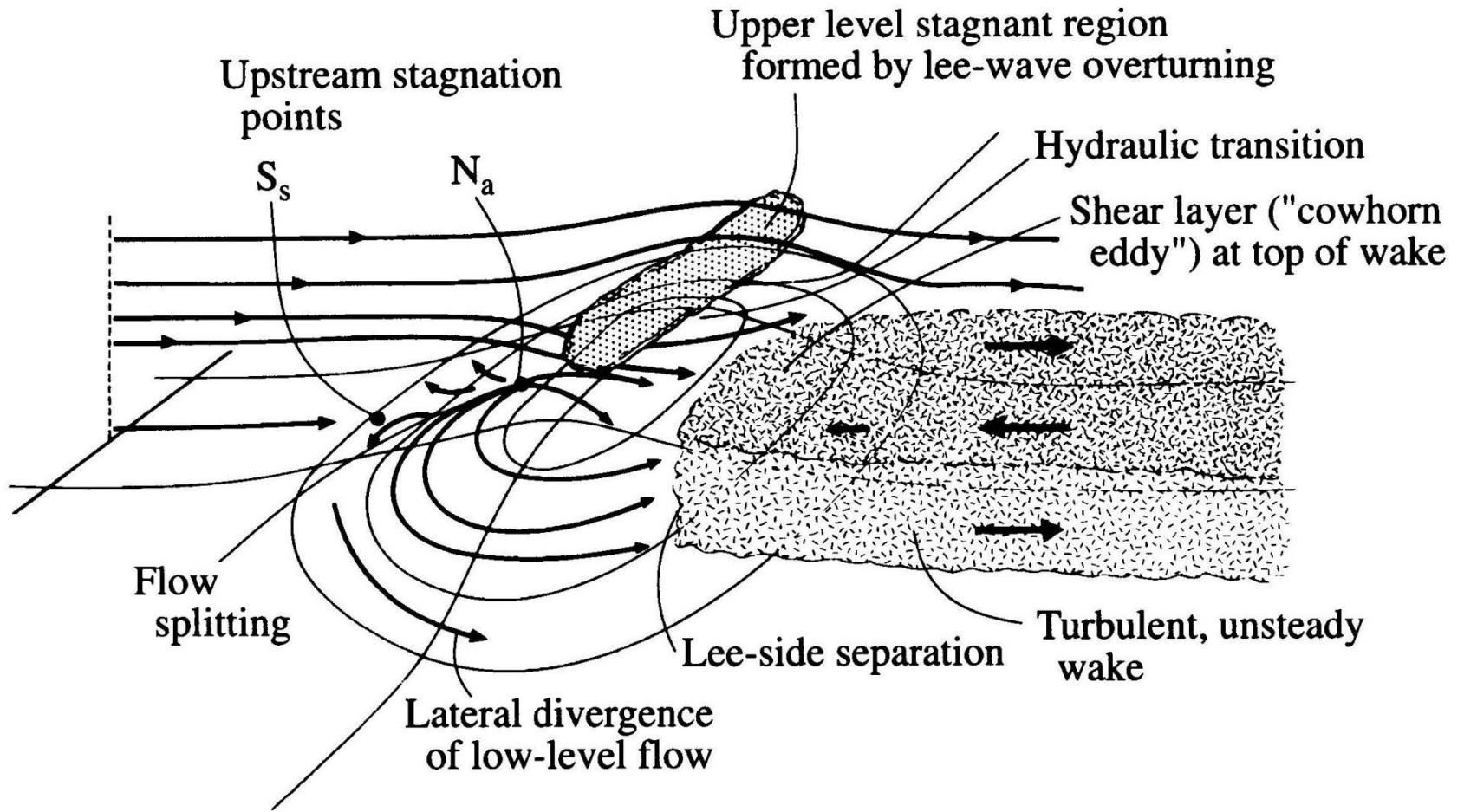


Fig. 6.28. Schematic diagram of the flow past a symmetrical obstacle where $Nh/U \gg 1$. Lines denote streamlines on the surface of the obstacle, and in the central plane of symmetry.

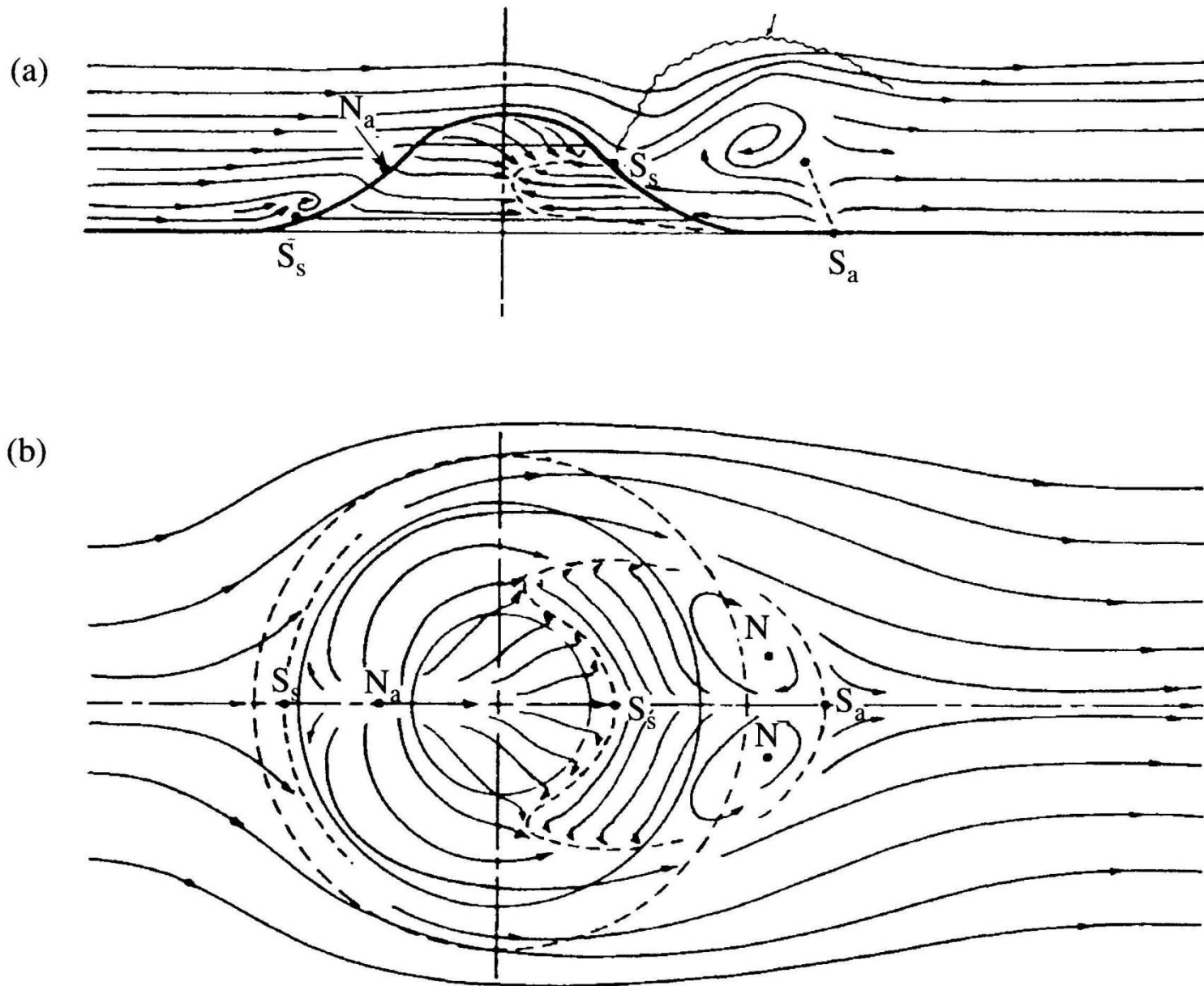


Fig. 6.26. As for Figure 6.24, but for $Nh/U = 2.5$. (From Hunt & Snyder 1980.)

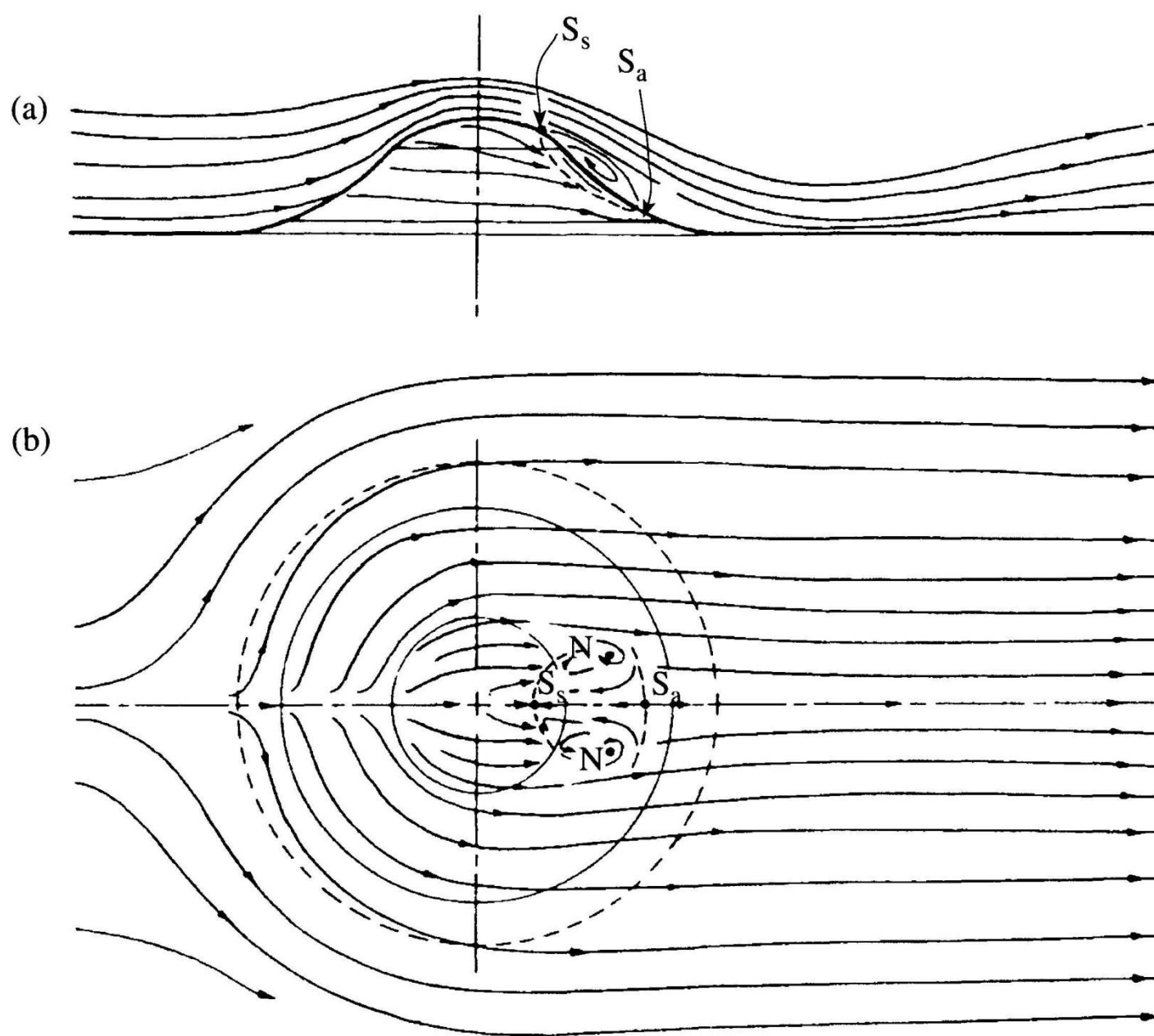
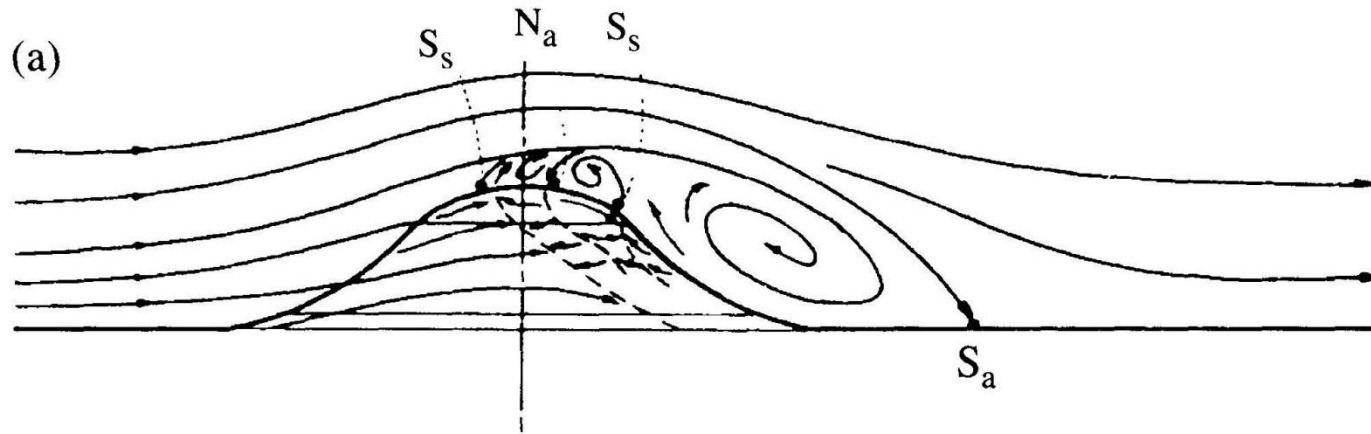
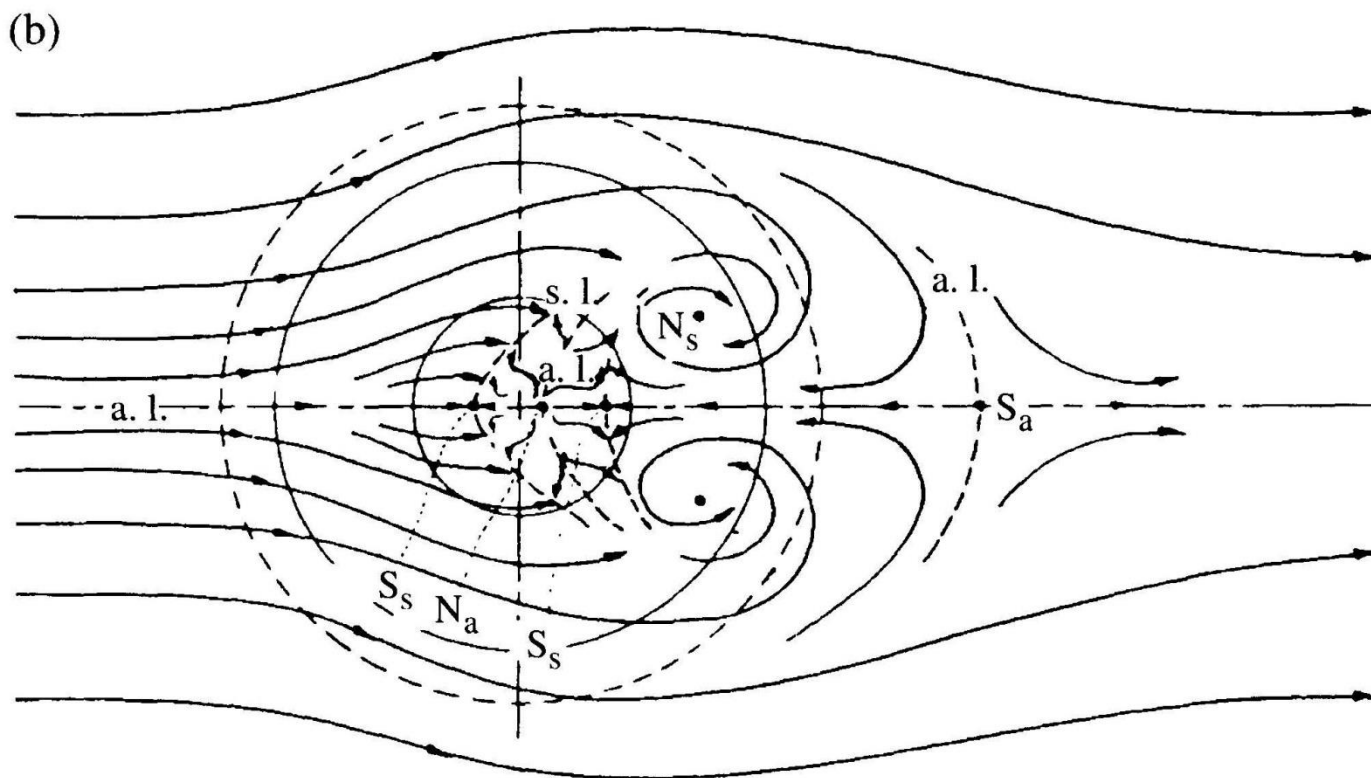


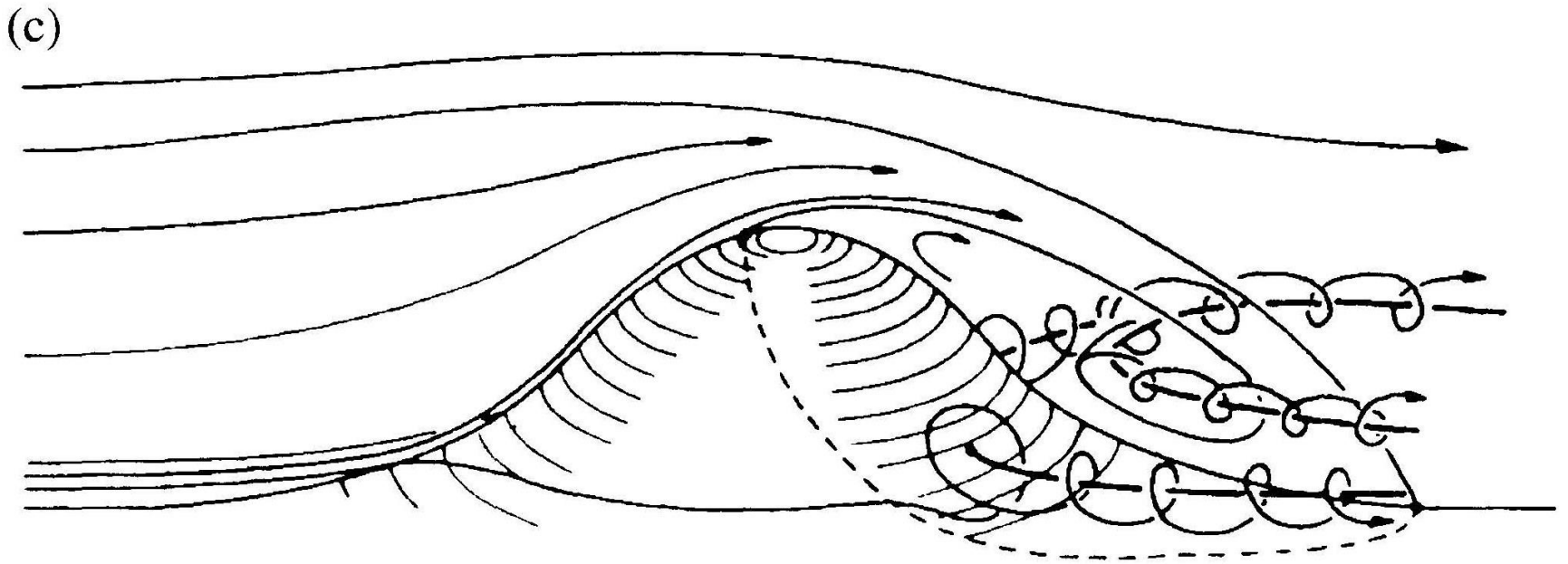
Fig. 6.25. As for Figure 6.24, but for $Nh/U = 1.0$. (From Hunt & Snyder 1980.)



$$N = 0$$



$N=0$



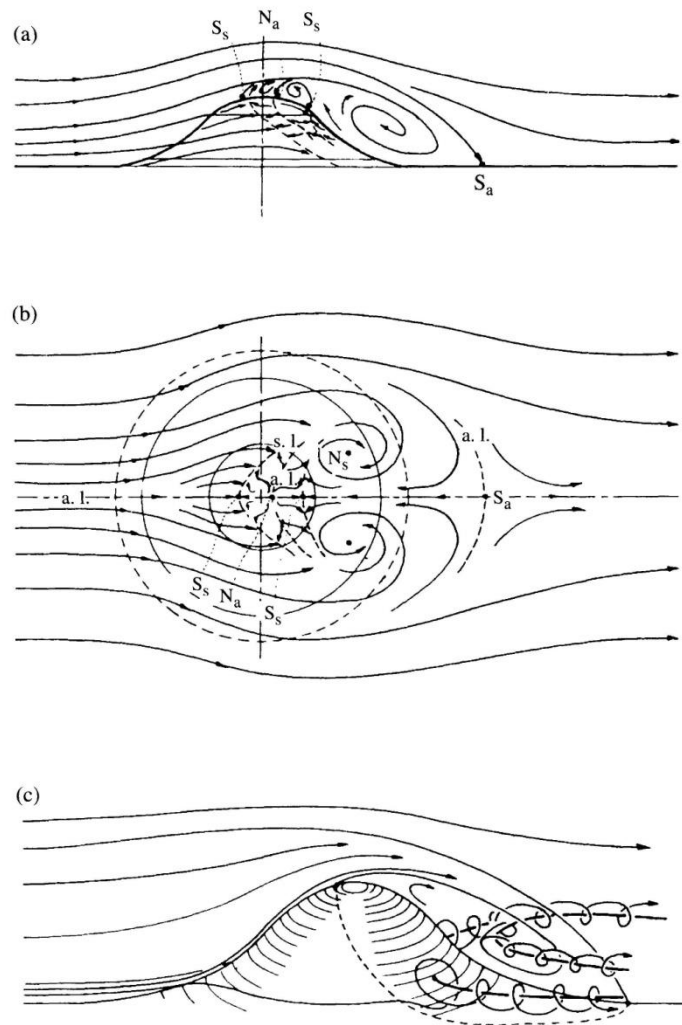


Fig. 6.22. (a) Side-view of the mean surface shear stress pattern and streamlines on the centre-plane of symmetry for homogeneous flow at large Reynolds number with a turbulent boundary layer, over an obstacle of the form (termed "polynomial hill" by Snyder *et al.* 1980)

$$z = h_m \left(\frac{1.04}{1 + \bar{r}^4} - \frac{0.083}{1 + (a\bar{r} - r_1)^2/a_1^2} - 0.03 \right),$$

where $\bar{r} = (x^2 + y^2)^{1/2}/a$, $h_m = a = 22.9$ cm, $r_1 = 20.3$ cm, $a_1 = 7.6$ cm. N_a , N_s , S_a , S_s denote nodes and saddle points of attachment and separation (see section 6.5). (b) As for (a) showing a plan view of the pattern of surface stress; a.l. and s.l. denote lines of attachment and separation respectively. (c) An inferred picture of the three-dimensional flow pattern of (a) and (b). An instantaneous flow may deviate considerably from this mean, particularly in the wake region. (From Hunt & Snyder 1980).

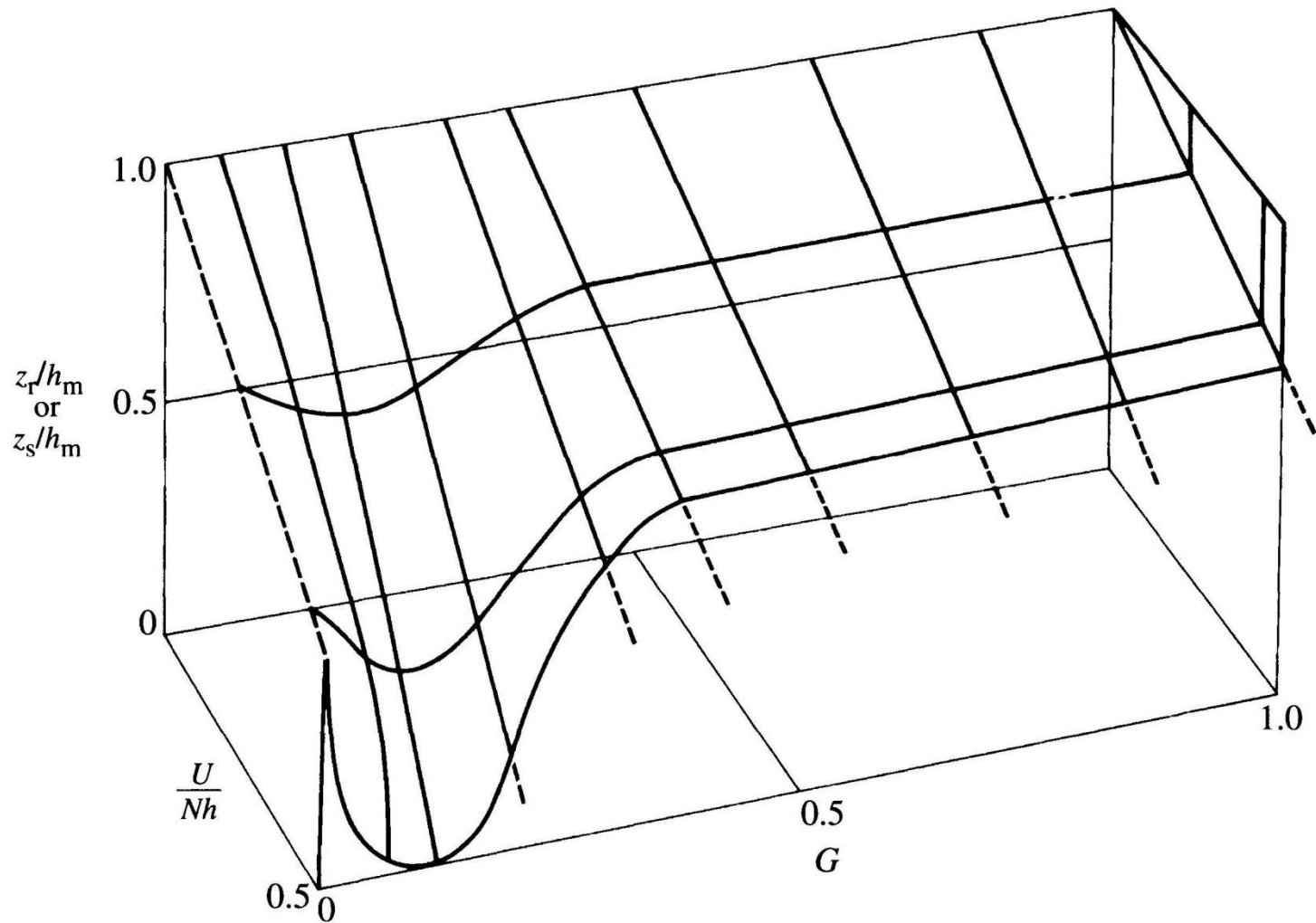


Fig. 6.41. The approximate observed upstream height of the dividing stream-surface z_r or z_s (i.e. the height of the highest streamline that does not pass over the barrier), observed upstream of the obstacle as in Figure 6.40, as a function of Nh/U and G . The figure is based on data with one obstacle shape, and should be seen as “schematic” until more data is available. For $G > 0.5$ the surface is depicted following (6.6.11). The surface is only shown for $Nh/U > 2$, with extensions indicated by dashed lines.

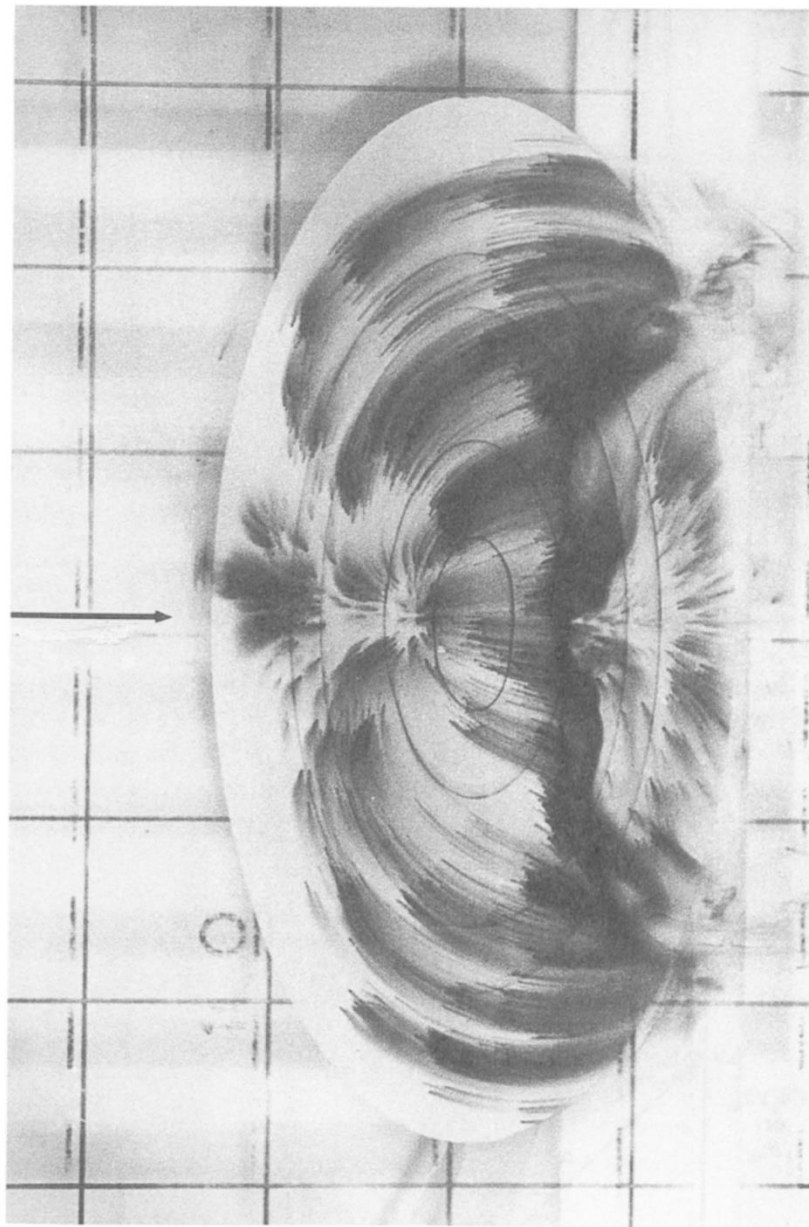


Fig. 6.34. Photograph of the surface flow pattern for an obstacle of the form (6.1.15) with $v = 3/2$, $b/a = 2$ and $Nh/U = 3.45$, visualised with dye emanating from small grains of potassium permanganate placed on the surface. Note the upstream stagnation points and flow-splitting, and the downstream wake.

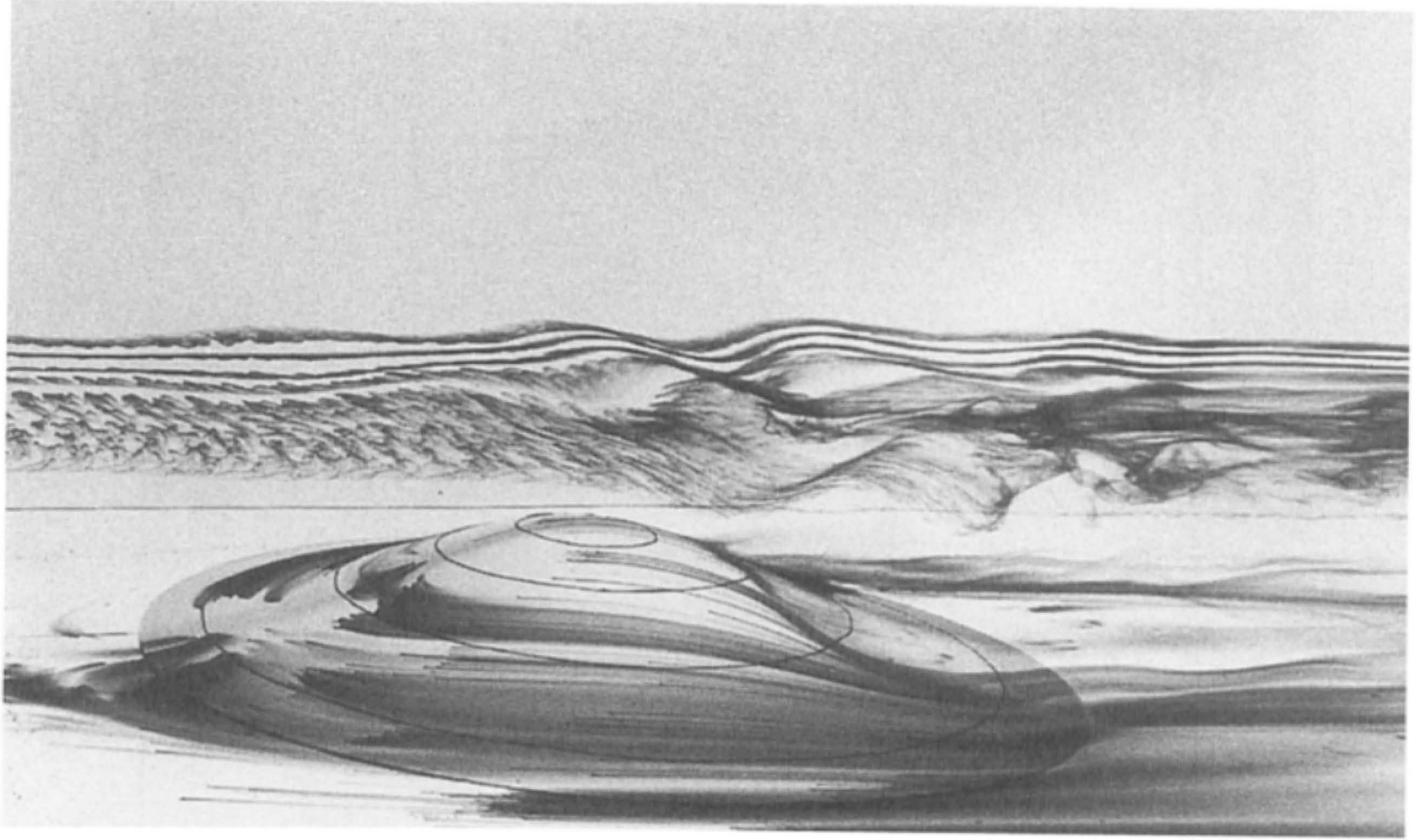


Fig. 6.35. The observed flow in the central plane of the obstacle of Figure 6.34, for $Nh/U = 2.5$. The flow is visualised by dye from a vertical rake placed upstream in the plane of symmetry, in addition to the dye released on the surface of the obstacle as in Figure 6.34.

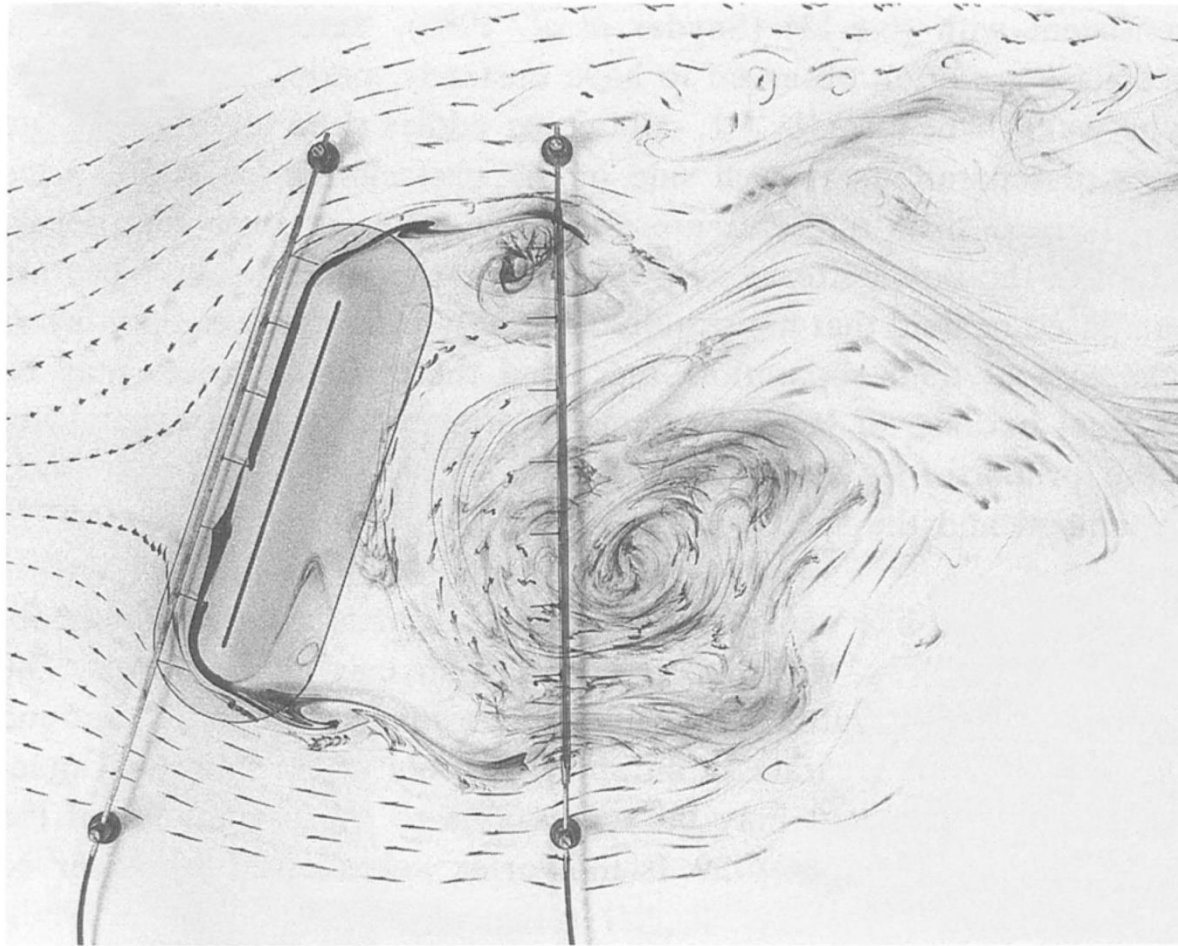


Fig. 6.38. The observed horizontal flow pattern at a height $z = h_m/3$ for uniformly stratified flow past a towed barrier inclined at 70° to the flow direction. $U/Nh = 0.1$, $Re = UL/\nu = 2990$, where L is the obstacle length. Flow visualisation is by neutrally buoyant dye released from three horizontal rakes: one upstream, one on the surface of the obstacle and one downstream. The dye released on the obstacle surface marks the vorticity produced there, and horizontal Kelvin-Helmholtz billows are evident after this dyeline separates. The vortices from these separated shear layers then become concentrated in lee-side vortices. The wake region is unsteady, with these unequal vortices being shed alternately. (From Baines 1990: reproduced by permission of ASCE.)